APPROXIMATE MAXIMUM LIKELIHOOD ESTIMATION IN LASER VELOCIMETRY.

Olivier Besson and Frédéric Galtier.

ENSICA, Department of Avionics and Systems.
1, Place Émile Blouin. 31056 Toulouse - France.
besson,galtier@ensica.fr

Abstract

In this paper, we study the estimation of signals of the form $s(t) = A.\exp\left\{-2\alpha^2 f_d^2 t^2\right\}.\cos(2\pi f_d t)$ *which are encountered in the measurement of particles velocity in a flow by means of laser Doppler velocimeters. We derive an Approximate Maximum Likelihood Estimator of the parameters* A *and* f_d *in the model considered. The algorithm is based upon replacing the first and second-order derivatives of the log-likelihood function by approximated and easy to compute expressions. Numerical examples illustrate the performance of the proposed method and quantify the influence of the sample size, the frequency* f_d *and the parameter* α*. They show that the estimator is statistically efficient in a wide range of scenarios.*

1. PROBLEM STATEMENT.

All the aerodynamic properties -lift, drag, etc....- of whichever airfoil -wing, fuselage or rotor blades- depend on the velocity of the air flow in which bath this profile. So, measuring accurately the speed of an air flow is necessary to study the aerodynamic performances of any profile. Since 1970, Laser Doppler Velocimetry has received considerable attention from fluid dynamicists. The efforts evolved toward the application of this instrumentation in different flow condition [1][2]. Laser velocimeters have proved to be useful in estimating particles velocity in a flow, when mechanical systems cannot be used because they may disturb the flow. As in any optical system, they provide a non-intrusive, reliable undisturbed way of measuring local velocities, and they allow remote measurements to be obtained from a very small probe volume with a fast response time. So far, the range of application of this kind of measurement system is very wide. It has already been used in fluid dynamic inside wind tunnels or in medicine to determine human blood velocity. Nowadays many flight control systems or on-board safety devices depend on the plane's speed. So, in aeronautic applications, it is essential to have a reliable way of measuring aircraft's speed. Moreover, the size and weight of the system in charge of this task is of primary concern. Until the late 1980's, laser velocimeters could not be used for aircraft applications, because of laser equipment size and speed requirements for signal processing. With the emergence of a new generation of cheap and small laser diodes, this principle becomes conceivable for on-board aeronautic applications. More specifically, we study a laser Doppler based system aimed at measuring aircraft speed. Towards this goal, two coherent laser beams are crossed and focused in the vicinity of the aircraft. They generate an interference fringe pattern composed of bright and dark fringes. As a particle of aerosol crosses the probe volume, it alternatively encounters equidistant bright and dark fringes. Then, according to Mie's backscattering Theory, light is scattered and the signal received in the photodetector is known to be of the form $A.\exp\left\{-2\frac{V^2}{W^2}t^2\right\}.\cos(2\pi\frac{V}{I}t)$ (see [3] for an approach by interference fringe model or [4] for an electromagnetic one). In the previous equation, A depends on the particle's size, V represents the particle's velocity (directly related to the aircraft speed), $2W$ is the total length of the probe volume and I is the interfringe width. In practice, only noisy measurements are available. Denoting $\alpha \triangleq \frac{I}{W}$ and $f_d \triangleq \frac{V}{I}$, *the problem at hand is to estimate the parameters* A and f_d *in the following model:*

$$\begin{aligned} x(t) &= A.s(t) + w(t) \\ &= A.\exp\left\{-2\alpha^2 f_d^2 t^2\right\}.\cos(2\pi f_d t) + w(t) \quad (1) \end{aligned}$$

for $t = 0, \pm 1, ..., \pm T$. In the above equation, $\{w(t)\}$ is assumed to be a sequence of i.i.d Gaussian variables with variance σ_w^2. Observe that, as the particle alternatively encounters bright and dark fringes, the frequency of the sinusoidal signal only depends on the particle's velocity and the interfringe width. Also, it should be pointed out that the Gaussian shape of the time-varying amplitude $e^{-2\alpha^2 f_d^2 t^2}$ is directly induced from the Gaussian shape of the intensity distribution within the laser beam.

2. APPROXIMATE MAXIMUM LIKELIHOOD ESTIMATION.

Maximum Likelihood estimators are generally of great interest as, under rather general conditions, they are known to be asymptotically efficient [5]. However, they generally lead to computational burdensome algorithms which may be an important drawback for real-time ap-

plications. In this section, we derive an Approximate Maximum Likelihood Estimator (noted AMLE) of the parameters A and f_d in the model (1). Starting from the exact ML estimator, we show that the first and second-order derivatives of the log-likelihood function can be accurately approximated by simple expressions. Using the latter in lieu of the formers in a Gauss-Newton (GN) procedure can therefore result in computational savings.

We first examine the exact MLE. Assuming that $w(t)$ is a white Gaussian noise, the pdf of $\mathbf{x} = [x(-T), ..., x(0), ..., x(T)]^T$ is given by:

$$p(\mathbf{x}, \boldsymbol{\theta}, \sigma_w^2) = \frac{1}{(2\pi\sigma_w^2)^{(2T+1)/2}} . \exp\left\{ -\frac{1}{2\sigma_w^2} \left\| \mathbf{x} - A\mathbf{s} \right\|^2 \right\} \quad (2)$$

where $\mathbf{s} = [s(-T), ..., s(0), ..., s(T)]^T$ and $\boldsymbol{\theta} = [A, f_d]^T$. The MLE is found by maximizing the log-likelihood function [5]:

$$\Lambda(\mathbf{x}, \boldsymbol{\theta}) = -\frac{2T+1}{2} \ln 2\pi - \frac{2T+1}{2} \ln \sigma_w^2 - \frac{1}{2\sigma_w^2} \left\| \mathbf{x} - A\mathbf{s} \right\|^2 \quad (3)$$

As the derivative of $\Lambda(\mathbf{x}, \boldsymbol{\theta})$ with respect to A is a linear function of this later, the value $\hat{A}$ which minimizes $\Lambda(\mathbf{x}, \boldsymbol{\theta})$, for any given value of f_d, is given by [5]:

$$\hat{A} = \frac{\mathbf{s}^T \mathbf{x}}{\mathbf{s}^T \mathbf{s}} \quad (4)$$

Reporting the previous equation in (3), the ML estimator of f_d can be found as the solution of the following minimization problem:

$$\hat{f}_d^{MLE} = \arg\left\{ \min_f \left[J_1(f) \right] \right\} \quad (5)$$

$$\text{with} \qquad J_1(f) = \left\| \mathbf{x} - \frac{\mathbf{s}^T \mathbf{x}}{\mathbf{s}^T \mathbf{s}} . \mathbf{s} \right\|^2 \triangleq \left\| \boldsymbol{\epsilon} \right\|^2 \triangleq \boldsymbol{\epsilon}^T \epsilon. \quad (6)$$

The minimization problem (5) can be solved by various techniques [6]. We choose here to implement a Gauss-Newton (GN) algorithm. Toward this end, the exact first-order derivative and approximated Hessian are to be calculated to iteratively minimize (6). The first-order derivative of (6) is given by:

$$\begin{aligned} J_1'(f) &= 2\boldsymbol{\epsilon}'^T \boldsymbol{\epsilon} \\ &= \frac{-2.\left(\mathbf{x}^T \mathbf{s}\right)}{\left(\mathbf{s}^T \mathbf{s}\right)^2} \begin{array}{l} \left\{ \left(\mathbf{x}^T \mathbf{s}_f'\right)\left(\mathbf{s}^T \mathbf{s}\right) \right. \\ \left. -2\left(\mathbf{x}^T \mathbf{s}\right)\left(\mathbf{s}^T \mathbf{s}_f'\right) \right\} \end{array} \end{aligned} \quad (7)$$

where $\mathbf{s}_f' \triangleq \frac{\partial \mathbf{s}}{\partial f}$ and derivation of $s(t)$ in (1) leads to:

$$s_f'(t) = -e^{-2\alpha^2 f_d^2 t^2} \left\{ 4\alpha^2 f_d t^2 \cos(2\pi f_d t) + 2\pi t \sin(2\pi f_d t) \right\} \quad (8)$$

The GN algorithm neglects the second order terms in the expression of the Hessian:

$$\begin{aligned} J_1''(f) &= 2\boldsymbol{\epsilon}'^T \boldsymbol{\epsilon}' + 2\boldsymbol{\epsilon}'^T \boldsymbol{\epsilon}'' \\ &\simeq 2\boldsymbol{\epsilon}'^T \boldsymbol{\epsilon}' \\ &= \frac{2}{\left(\mathbf{s}^T \mathbf{s}\right)^2} . \begin{array}{l} \left\{ \left(\mathbf{x}^T \mathbf{s}_f'\right)^2 \left(\mathbf{s}^T \mathbf{s}\right) \right. \\ -2\left(\mathbf{x}^T \mathbf{s}\right)\left(\mathbf{x}^T \mathbf{s}_f'\right)\left(\mathbf{s}^T \mathbf{s}_f'\right) \\ \left. +\left(\mathbf{x}^T \mathbf{s}\right)^2 \left(\mathbf{s}_f'^T \mathbf{s}_f'\right) \right\} \end{array} \end{aligned} \quad (9)$$

Therefore, each iteration of the GN algorithm requires the computation of $\mathbf{x}^T\mathbf{s}, \mathbf{x}^T\mathbf{s}_f', \mathbf{s}^T\mathbf{s}, \mathbf{s}^T\mathbf{s}_f'$ and $\mathbf{s}_f'^T\mathbf{s}_f'$. *The idea of the approximate MLE (AMLE) is to replace* $\mathbf{s}^T\mathbf{s}, \mathbf{s}^T\mathbf{s}_f'$ and $\mathbf{s}_f'^T\mathbf{s}_f'$ *in* $J_1'(f), J_1''(f)$ *by approximated and directly computable expressions.* Hence, only $\mathbf{x}^T\mathbf{s}$ and $\mathbf{x}^T\mathbf{s}_f'$ need to be computed, which results in significant computational savings ($\approx$ from $5(2T+1)$ mul/add to $2(2T+1)$). For T large (as $e^{-2\alpha^2 f_d^2 t^2} \cos(2\pi f_d t)$ decreases very quickly, this is not a restrictive condition), $\mathbf{s}^T\mathbf{s}, \mathbf{s}^T\mathbf{s}_f'$ and $\mathbf{s}_f'^T\mathbf{s}_f'$ can be accurately approximated by $\lim_{T\to\infty} \mathbf{s}^T\mathbf{s}$, $\lim_{T\to\infty} \mathbf{s}^T\mathbf{s}_f'$ and $\lim_{T\to\infty} \mathbf{s}_f'^T\mathbf{s}_f'$. From (1) and (8), these expressions will consist of a combination of terms with the following forms:

$$\begin{matrix} S_c \\ S_s \end{matrix} = \lim_{T\to\infty} \sum_{t=-T}^{T} e^{-4\alpha^2 f_d^2 t^2} . t^n . \begin{matrix} \cos \\ \sin \end{matrix} (4\pi f_d t) . \quad (10)$$

S_c and S_s are normally convergent series. But they do not admit analytical expressions as a function of α, f_d, n. However (10) can be viewed as a rectangular approximation of an integral. So, to get further insights into their values, we propose to use the following type of approximation :

$$\begin{aligned} &\lim_{T\to\infty} \sum_{t=-T}^{T} \exp\left\{ -4\alpha^2 f_d^2 t^2 \right\} . t^n . \begin{matrix} \cos \\ \sin \end{matrix} (4\pi f_d t) \\ \simeq &\int_{-\infty}^{\infty} \exp\left\{ -4\alpha^2 f_d^2 u^2 \right\} . u^n . \begin{matrix} \cos \\ \sin \end{matrix} (4\pi f_d u) . du \end{aligned} \quad (11)$$

The right-hand sides of (11) correspond to a Continuous Time Fourier transform whereas the left-hand sides are the Discrete Time Fourier Transform counterparts. Based upon (11), it was shown in [7] that:

$$\begin{aligned} \lim_{T\to\infty} \mathbf{s}^T\mathbf{s} &\simeq \frac{\sqrt{\pi}}{4\alpha f_d} \\ \lim_{T\to\infty} \mathbf{s}^T\mathbf{s}_f' &\simeq -\frac{\sqrt{\pi}}{8\alpha f_d^2} \\ \lim_{T\to\infty} \mathbf{s}_f'^T\mathbf{s}_f' &\simeq \frac{\sqrt{\pi}.\left(3\alpha^2 + 2\pi^2\right)}{16\alpha^3 f_d^3} \end{aligned} \quad (12)$$

These approximations allow to represent the products of the signal's model vectors as simple analytical expressions. Thus, it remains to calculate the products $\mathbf{x}^T\mathbf{s}$ and $\mathbf{x}^T\mathbf{s}_f'$. Replacing $\mathbf{s}^T\mathbf{s}, \mathbf{s}^T\mathbf{s}_f'$ and $\mathbf{s}_f'^T\mathbf{s}_f'$ by their approximated values (12), we get:

$$\tilde{J}_1'(f) \simeq \frac{-4\alpha}{\sqrt{\pi}} . \left\{ 2f . \left(\mathbf{x}^T \mathbf{s}_f'\right) + \left(\mathbf{x}^T \mathbf{s}\right) \right\} . \left(\mathbf{x}^T \mathbf{s}\right) \quad (13)$$

$$\tilde{J}_1''(f) \simeq \frac{2}{\sqrt{\pi}.\alpha f} . \begin{array}{l} \left\{ \alpha^2 . \left[2f . \left(\mathbf{x}^T \mathbf{s}_f'\right) + \left(\mathbf{x}^T \mathbf{s}\right) \right]^2 \right. \\ \left. +2\left(\mathbf{x}^T \mathbf{s}\right)^2 . \left[\alpha^2 + \pi^2\right] \right\} \end{array} \quad (14)$$

From (13) and (14) and according to the GN algorithm, the Approximate MLE iteratively updates the frequency as:

$$\hat{f}^{(n+1)} = \hat{f}^{(n)} - \left[\frac{\tilde{J}_1'(f)}{\tilde{J}_1''(f)}\right]_{\hat{f}^{(n)}} \qquad (15)$$

The iterations are stopped whenever $\left|\hat{f}^{(n+1)} - \hat{f}^{(n)}\right| \leq \delta \left|\hat{f}^{(n)}\right|$ where δ is a user defined parameter. It should be observed that formulas (13) and (14) are *asymptotically approximated* expressions. Therefore, the AMLE is expected to perform well only for T large enough. A coarse search for the maximum of the periodogram can be used to initialize the algorithm. The numerical examples of next section demonstrate that this initialization method is enough accurate to avoid possible convergence towards a local minimum.

3. NUMERICAL EXAMPLES AND CONCLUDING REMARKS.

In this section, we provide numerical illustrations of the performance of the estimator under study and compare it with the Cramér-Rao Bounds [7]. For each figure shown, 500 Monte-Carlo simulations were run to estimate the Mean-Square Error (MSE) of the estimator. In the figures below, the parameter α is given as $\alpha = 0.122857$, the Signal to Noise Ratio $SNR \stackrel{\triangle}{=} \frac{A^2}{2\sigma_w^2} = 15dB$, and $A = 1$. Figure 1 studies the influence of the sample size T:

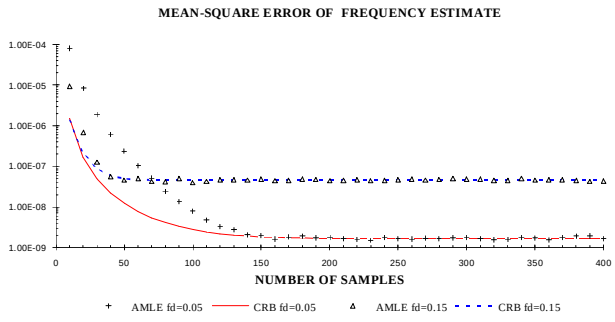

Fig.1: CRB and performance of AMLE versus T. $SNR = 15dB$. $f_d = 0.05$ or $f_d = 0.15$. $A = 1$.

As can be seen from this figure, the AMLE is very close to the CRB, at least for a sufficient number of samples ($T = 140$ for $f_d = 0.05$, $T = 30$ for $f_d = 0.15$). This is expected as formulas (12) are asymptotic in T (as $\exp\left\{-2\alpha^2 f_d^2 t^2\right\}$ decreases very quickly, (12) holds for reasonable values of T). In fact, many other simulations demonstrated that the AMLE yields good performances as long as $T \geq T_{opt}$; where $T_{opt} = \frac{1}{\alpha f_d}$. This is due to the fact that, for t larger than T_{opt}, the signal essentially contains noise, because $\exp\left\{-2\alpha^2 f_d^2 t^2\right\} \approx 0$. It can be seen that $T \geq T_{opt}$ corresponds to the case where *all the useful signal inside the probe volume* $2W$ has been recorded.

Figures 2, 3 and 4 investigate the respective influences of f_d, α and SNR onto the performance of the estimator. For the following simulation results reported here, the number of samples T of the signal has been chosen such that $T \geq T_{opt}$.

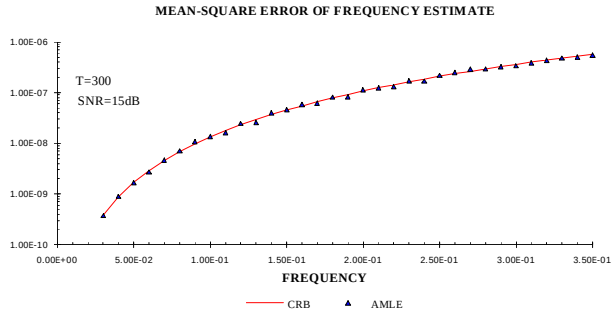

Fig.2: CRB and performance of AMLE versus f_d. $T = 300$. $SNR = 15dB$. $A = 1$.

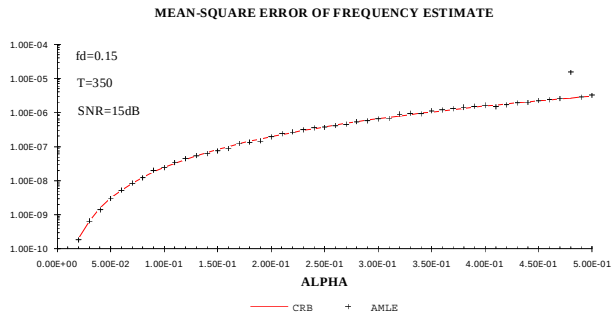

Fig.3: CRB and performance of AMLE versus α. $T = 300$. $SNR = 15dB$. $A = 1$. $f_d = 0.15$.

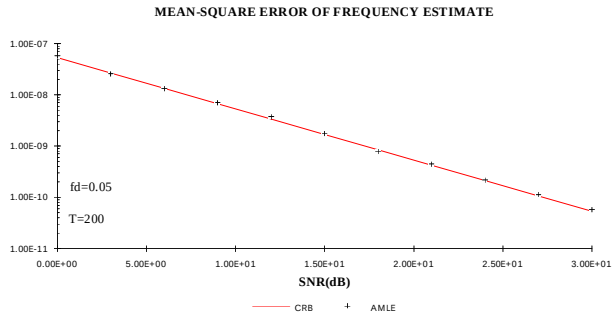

Fig.4: CRB and performance of AMLE versus SNR. $T = 300$. $SNR = 15dB$. $A = 1$. $f_d = 0.05$.

In conclusion, the estimator proposed herein achieves computational simplicity and is shown to be statistically efficient (at least for T large enough, *i.e.* $T \geq T_{opt}$) over a wide range of scenarios (versus large f_d, α and SNR' domains).

In the previous simulations, the stop parameter δ was chosen equal to 5.10^{-4}. However, in a series of simulations not reported here, it was observed that δ can be chosen up to 3.10^{-2} without increasing the MSE. This choice reduces of 1.5 the average number of iterations of the AMLE's algorithm.

We now illustrate the performance of the AMLE when applied to real data. The laser Doppler system was placed in a wind tunnel aerosolized with a known velocity. The signal received by the photodetector was stored for post-treatment. The AMLE was applied to the recorded data. A search of the maximum of the FFT was used to initialized the ML and AML estimators. The frequencies estimated by the MLE and the FFT are also reported to compare the results of the AMLE with that of the exact maximum likelihood and of the simple FFT method. Figures 5 and 7 show the time representation of the signal. Figures 6 and 8 plot the frequencies determined by these three estimators versus the number of signal's samples taken into account.

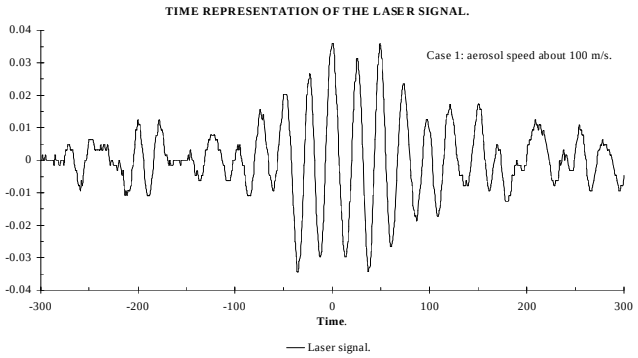

Fig.5: Time representation of a real laser signal. Case 1.

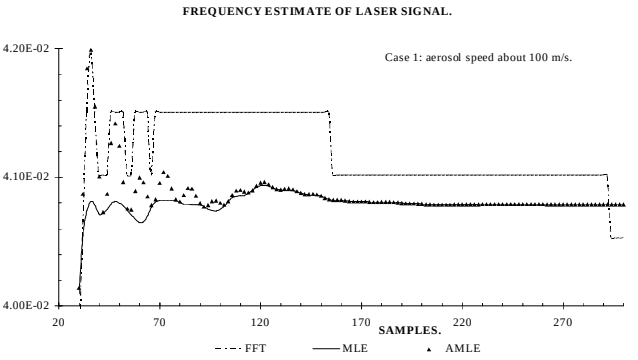

Fig.6: Frequency estimated by AML, ML, and max. of FFT estimators applied to real laser signal versus T.

The second case illustrates the robustness of the AMLE algorithm with respect to defects in the optical system, leading to a non-symmetric interfringe pattern (see Figures 7 and 8).

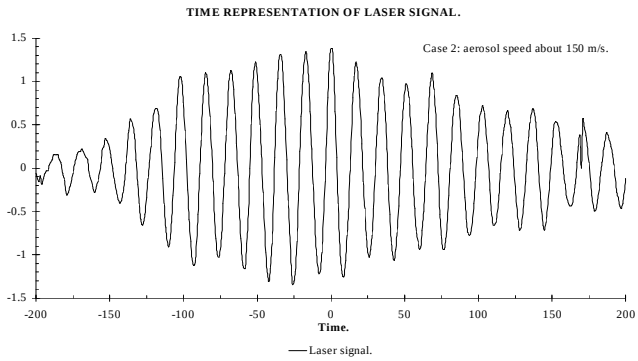

Fig.7: Time representation of a real laser signal. Case 2.

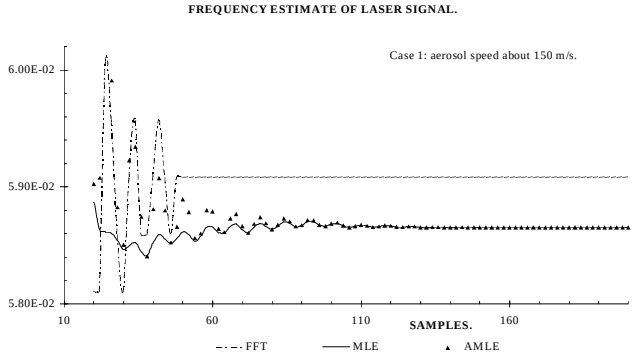

Fig.8: Frequency estimated by AML, ML and max. of FFT estimators applied to real laser signal versus T.

It can be seen from these four figures above that for sufficiently large T the AMLE applied to real laser signals *determines exactly* the same frequency than the exact ML estimator, requiring less computational time.

Acknowledgment: This work is supported by Sextant Avionique under contract n°1432411944164.

References

[1] M. Riethmuller, "Laser doppler velocimetry", in *Measurement of unsteady fluid dynamic phenomena* (B.E.Richards, Editor), Mc Graw Hill, 1977.

[2] *Laser Velocimetry,* in Lecture Series of the von Karman Institute for fluid dynamics, September 1981.

[3] P.D. Lax and R.S. Phillips, *Scattering Theory*, Academic Press, New-York, 1967.

[4] A. Coghe and U. Ghezzi, "LDA Signal Analysis", *Proceedings of the Dynamic Flow Conference*, Skovlunde (DK), 1979.

[5] S. Kay, *Fundamentals of Statistical Signal Processing: Estimation Theory,* Prentice Hall, Englewood Cliffs, 1993.

[6] R. Fletcher, *Practical Methods of Optimization*, John Wiley & Sons, New-York, 1987.

[7] O. Besson and F. Galtier, "Bounds for estimation of particle's velocity from laser measurements", *Proceedings SSAP96*, Corfu, June 1996.